Follow us @BoneJointRes

Freely available online OPEN ACCESS

BJR

BONE FRACTURE

# The role of intermittent PTH administration in conjunction with allogenic stem cell treatment to stimulate fracture healing

**L. Osagie-Clouard,**
**R. Meeson,**
**A. Sanghani-Kerai,**
**M. Bostrom,**
**T. Briggs,**
**G. Blunn**

*From University College London, London, UK*

## Aims

A growing number of fractures progress to delayed or nonunion, causing significant morbidity and socioeconomic impact. Localized delivery of stem cells and subcutaneous parathyroid hormone (PTH) has been shown individually to accelerate bony regeneration. This study aimed to combine the therapies with the aim of upregulating fracture healing.

## Methods

A 1.5 mm femoral osteotomy (delayed union model) was created in 48 female juvenile Wistar rats, aged six to nine months, and stabilized using an external fixator. At day 0, animals were treated with intrafracture injections of 1 × $10^6$ cells/kg bone marrow mesenchymal stem cells (MSCs) suspended in fibrin, daily subcutaneous injections of high (100 µg/kg) or low (25 µg/kg) dose PTH 1-34, or a combination of PTH and MSCs. A group with an empty gap served as a control. Five weeks post-surgery, the femur was excised for radiological, histomorphometric, micro-CT, and mechanical analysis.

## Results

Combination therapy treatment led to increased callus formation compared to controls. In the high-dose combination group there was significantly greater mineralized tissue volume and trabecular parameters compared to controls (p = 0.039). This translated to significantly improved stiffness (and ultimate load to failure (p = 0.049). The high-dose combination therapy group had the most significant improvement in mean modified Radiographic Union Score for Tibia fractures (RUST) compared to controls (13.8 (SD 1.3) vs 5.8 (SD 0.5)). All groups demonstrated significant increases in the radiological scores – RUST and Allen score – histologically compared to controls.

## Conclusion

We demonstrate the beneficial effect of localized MSC injections on fracture healing combined with low- or high-dose teriparatide, with efficacy dependent on PTH dose.

Cite this article: *Bone Joint Res* 2021;10(10):659–667.

**Keywords:** Fracture healing, Teriparatide, Stem cells

## Article focus

- Bone formation with locally injected mesenchymal stem cells (MSCs).
- Combination effects of MSCs and parathyroid hormone (PTH).

## Key messages

- The combination of subcutaneous PTH and local MSCs increases fracture healing in a nonunion model.
- The combined interventions have an improved effect.

## Strengths and limitations

- Our study highlights the importance of both therapies individually and in combination, with possible clinical impact.
- Further investigation of the underlying mechanistic pathways is needed.

Correspondence should be sent to Anita Sanghani-Kerai; email: anitas@fitzpatrickreferrals.co.uk

doi: 10.1302/2046-3758.1010.BJR-2019-0371.R2

*Bone Joint Res* 2021;10(10):659–667.

## Introduction

Teriparatide (parathyroid hormone (PTH) 1-34) is the N-terminal fragment of the intact 84-amino acid polypeptide hormone and is approved for the treatment of osteoporosis in both the USA and Europe.[1] Despite a large body of clinical work demonstrating the utility of PTH for increasing bone density, its use as a pharmacological adjunct to fracture healing has predominantly been in the preclinical setting,[2-6] where such studies have demonstrated beneficial effects on callus formation, with increased trabeculae and an accelerated remodelling phase. Clinically, PTH has been shown to accelerate radiological healing of distal radii fractures in the osteoporotic population, improve the healing of pelvic ring fractures, and accelerate healing in both sternal and humeral non-/delayed unions.[7-11] Yet, conversely, prospective trials using teriparatide for post sub-/peritrochanteric hip fractures have not yielded promising results.[12,13]

As research into pharmacological adjuncts to improve fracture healing has grown, so too has the investigation into the use of biological factors to accelerate bone formation. Both systemically administered and locally delivered autologous mesenchymal stem cells (MSCs) have been used in preclinical models to enhance fracture healing. Patient case series have also demonstrated the utility of locally delivered stem cells in the treatment of tibial and calcaneal nonunions.[14-17]

The PTH anabolic effect is in part due to its ability to induce the osteoblast transcription factors Osterix (OSX) and Runt-related transcription factor 2 (Runx2) in MSCs. The combined use of PTH with stem cells in fracture healing has been examined. Groups have used intravenous injections of bone marrow-derived cells with systemic PTH 1-34 to heal rodent rib fractures, with significant increases in mineralized callus formation by six weeks compared to controls.[18] Positive findings were also reported in the treatment of spinal fractures, again with intravenous MSCs and systemic PTH, although the concentrations used were significantly higher than those which would be used clinically.[19] Interestingly, very little work has explored the use of locally delivered MSCs and systemic PTH. This study uses the anabolic effect of teriparatide with MSCs delivered in fibrin glue[20] to administer cells intralesionally directly into the fracture. As such, we hypothesized that the administration of locally delivered MSCs suspended in fibrin glue, in combination with systemic PTH treatment at varying doses, will lead to enhanced fracture healing in a rat delayed union fracture model compared to an untreated control group or rats treated with MSCs or PTH only.

## Methods

**Cell isolation.** Rat bone marrow mesenchymal stem cells (rBMSCs) were harvested from two- to four-week-old female Wistar rat femora (189 g to 228 g). All animal work was completed in accordance with the UK Home Office Animals Scientific Procedures Act of 1986 and were approved by the relevant Animal Welfare Ethical Review Board and UK Home Office approved Personal and Project licence (PPL 70/8247). rBMSCs were characterized using trilineage differentiation and flow cytometery (CytoFLEX; Beckman Coulter, UK) at passage 3, whereby 30,000 cells per group were fixed and assessed using a combination of positive CD90 (Anti-Mouse/Rat CD90.1 (Thy-1.1); eBioscience, UK) and CD29 (Anti-Mouse/Rat CD29 (Integrin β 1); eBioscience), and negative MSC markers CD45 (Anti-Rat CD45; eBioscience) and CD34 (Anti-CD34; Abcam, UK) and compared with appropriate isotype controls.[21] An ARRIVE checklist is included in the Supplementary Material to show that the ARRIVE guidelines were adhered to in this study.

Prior to the surgical model, an in vitro study was conducted to assess cell viability in fibrin glue and the resultant viscosity of the cell/fibrin suspension. A total of 100,000 passage 3 rBMSCs were suspended in 1 ml of the combined fibrin glue and passed through a 25 G needle. Cells were easily passed through the needle within 15 seconds, after which a gelatinous pliable clot formed. At day seven, cell viability was confirmed with calcein AM live dead staining (Figure 1e). In the surgical procedure, rBMSCs at passage 3 from three rats were pooled together before being introduced into the fracture site to eliminate cell variability.

PTH was prepared to a concentration of 25 µg/kg (low dose) and 100 µg/kg (high dose) by dissolving it in 0.9% saline, mannitol, and monosodium phosphate (MilliporeSigma, UK) before sterile filtration and administered subcutaneously day after surgery, and then every 48 hours for five weeks until the rats were euthanized. The injection site was changed daily.

**Surgical procedure.** A total of 48 female Wistar rats, weighing 203 g to 232 g and aged between six and nine months, underwent gaseous anaesthesia. Using anatomical landmarks and a custom precision jig-guide system,[22] four bicortical threaded 1.4 mm stainless steel fixator pins were placed in the craniomedial femur. Pins exited through separate stab incisions and the custom variable spacing fixator was attached. A mid-diaphyseal femoral osteotomy, with no periosteal stripping, was made using a diamond tipped handsaw. A spacer ensured a fixed offset of 5 mm, the fixator was then attached and the osteotomy gap distracted to 1.5 mm for all the rats (Figures 1a to 1d). The facia overlying the biceps femoris-was closed using a mattress suture and then the skin was closed using a sub-cutaneous continuous suture. This model has demonstrated delayed union at weeks when assessed without intervention.[23]

Animals were housed in pairs without dietary or ambulation restrictions on a standard rodent diet; cages included adequate bedding and unrestricted access to fluids, along with objects for animal enrichment. Animals were randomized into six equal groups (n = 8 per group) as follows: 1) empty gap; 2) rBMSCs within gap; 3) low-dose PTH injections; 4) rBMSCs within gap and low-dose

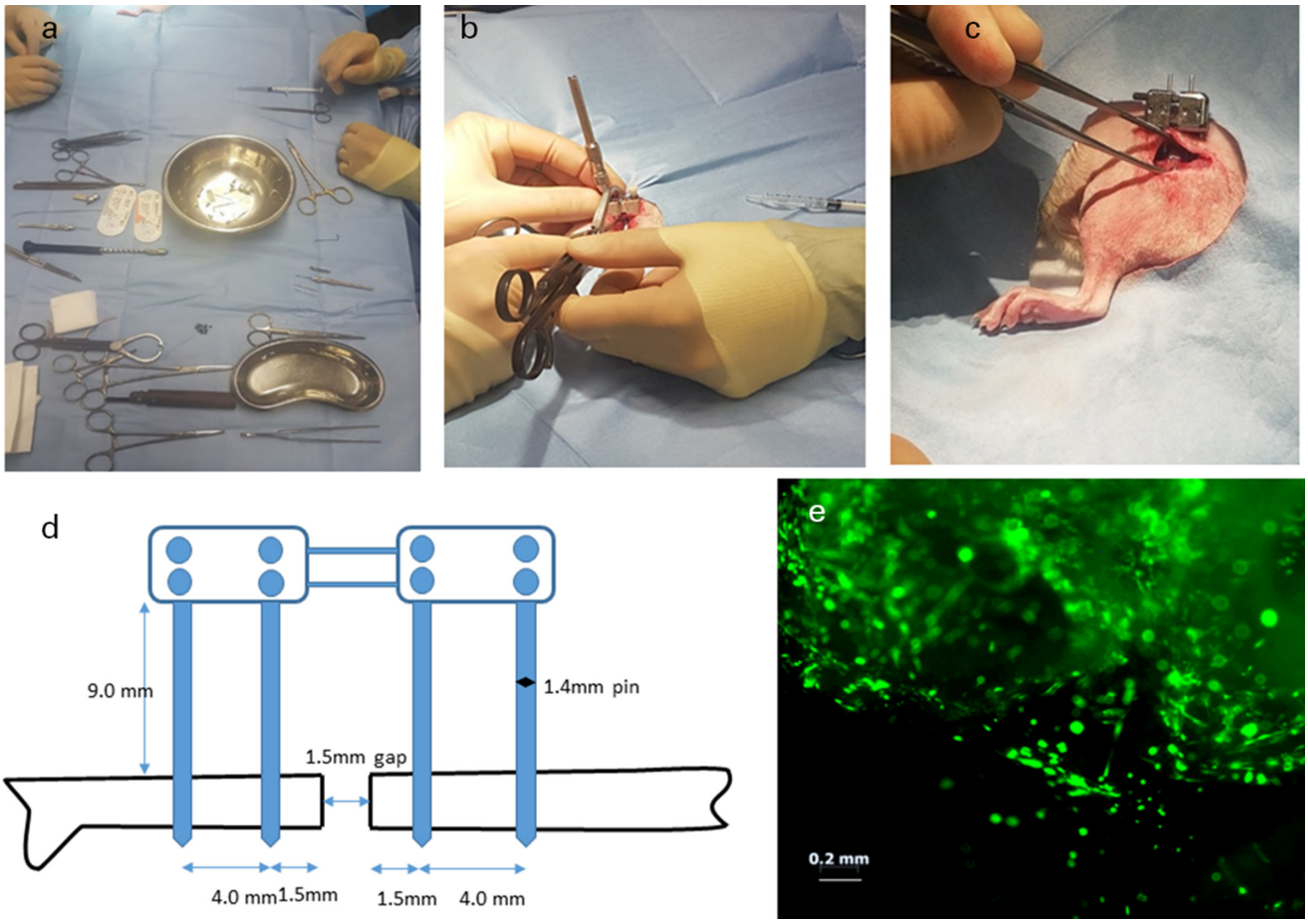


Fig. 1

a) Photographs of surgical instruments required, b) intraoperative image of pin placement, and c) intraoperative image of fixator prior to wound closure; d) fluorescent microscope image of cells stained with live-dead in fibrin glue; e) a pictorial representation of the ex-fixator system.

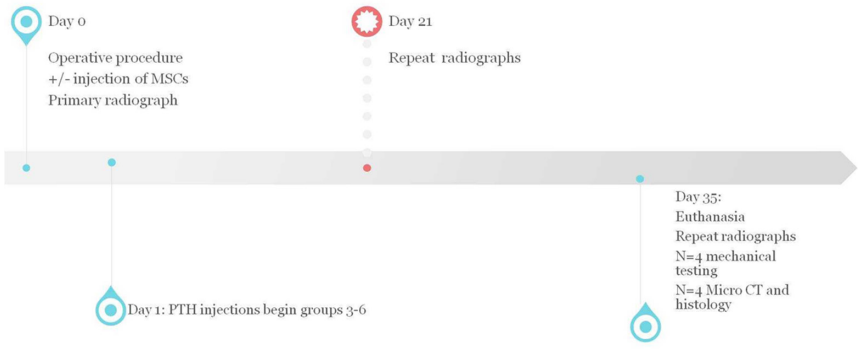


Fig. 2

A schematic diagram demonstrating the experimental set-up and overall time line of the surgeries to euthanasia. MSC, mesenchymal stem cell; PTH, parathyroid hormone.

PTH injections; 5) high-dose PTH injections; and 6) rBMSCs within gap and high-dose PTH injections.

For groups requiring rBMSC injections, rBMSCs were trypsinized and combined with the thrombin component of the fibrin glue on the day of surgery. Once the surgical procedure was complete and skin closed, the thrombin containing cell solution was mixed with the fibrinogen component and injected intralesionally using a 25 G needle into the fracture gap at a concentration of $1 \times 10^6$ cells/kg through the skin. As such, $1 \times 10^6$ cells/kg was used as per Chamieh et al.[24] During all surgical procedures, following the creation of the osteotomy, care was taken not to overirrigate the surgical field so as not to remove any forming haematoma.

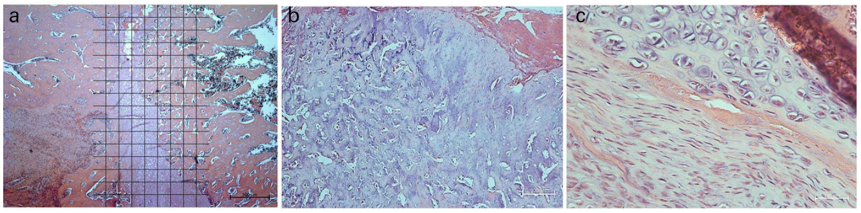


Fig. 3

Histological slides with haematoxylin and eosin staining, demonstrating fracture gap and overlying grid used for histomorphometeric analysis at: a) 2.5× magnification; b) 10× magnification; and c) 50× magnification.

An empty gap served as a control; similar works have demonstrated negligible effect of fibrin glue alone on fracture healing over a comparable time period, as no such fibrin-only group was used (Figure 2).[20] Five weeks post-surgery, all rats were euthanized with $CO_2$ and euthanasia was confirmed using cervical dislocation.

**Radiological analysis.** All animals underwent radiographs of the operated limb in two orthogonal planes immediately post-procedure, at three weeks, and post-euthanasia at five weeks. The radiographs were then scored using a modified Radiographic Union Score for Tibia fractures (RUST).[25] This score was used over the standard RUST,[26] as it provides a greater scale in order to better delineate partial and absolute union, and was more appropriate than a Lane-Sandhu,[27] as one would expect very few instances of score IV healed and remodelled over this experimental timeframe.

**Micro-CT analysis.** Micro-CT was performed posteuthanasia (n = 4 per group), femora were dissected en mass, and soft-tissue attachments removed; they were then fixed in formalin with the fixator in situ. All samples were scanned and analyzed using the same settings and categories. During the scanning process, the samples were wrapped in cling film and placed on a sample holder. The entire femur was scanned, and then the region of interest (ROI) was centred over the fracture gap to avoid beam-hardening artefact from the presence of the fixator pins. In order to analyze the callus in each slice included in the ROI, a shrink wrap protocol was used to stretch over holes < 40 pixels.[22]

Micro-CT scans were reconstructed using NRecon (Bruker, Belgium) with smoothing = 2, ring artefact reduction = 12%, and beam hardening artefact = 41%. Analysis was performed with CTAn (Bruker). Using the measuring tool, the centre point of the osteotomy was determined and the transverse slice at that point was selected as the reference slice. The callus was isolated using a 2D ROI shrink wrap stretching over holes < 40 pixels, despeckled < 150 voxels, and then 3D analysis was performed. The central 60% of the osteotomy gap, with 180 × 5 um slices, i.e. only new bone formation within the osteotomy was analyzed for each size. Callus was deemed as any tissue formed between the two cut surfaces of the femur; mineralized callus was determined by thresholding with a lower grey threshold of 100, and an upper grey threshold of 255. Unmineralized callus was also quantified, excluding the medullary regions, by manual delineation, performed at one in every ten resampled coronal slices through the volume of interest. Images then underwent 3D analysis for the following parameters: 1) bone volume (BV); 2) bone volume fraction (BV/TV); 3) trabecular number (TbN); and 4) trabecular thickness (TbTh).

**Histology and histomorphometry analysis.** Following CT analysis, fixators were removed and specimens were fixed in 10% buffered formaldehyde, and decalcified in ethylenediaminetetraacetic acid (EDTA). Decalcification was confirmed by radiography. Following dehydration, de-fatting, and sectioning, slides were dewaxed, rehydrated, and stained in haematoxylin, then counterstained with eosin. Three slides per specimen were also graded using the Allen score[28] as follows: Grade '0' nonunion (fibrous tissues), '1' incomplete cartilage union (cartilage with some fibrous tissues), '2' complete cartilage union (entirely cartilage), '3' incomplete bony union with early ossification phase (predominantly cartilage with some trabecular bone), '4' incomplete bony union with intermediate ossification phase (equal amounts of cartilage and trabecular bone), '5' incomplete bony union with late ossification phase (predominantly trabecular bone with some cartilage), and '6' complete bony union (entirely bone).

Slides also underwent histomorphometric analysis. Slides were observed under a light microscope (KS-300; Zeiss, UK) at 2.5× magnification was performed on the most central slice, using a line-intercept method with a grid scaled to the graticule drawn using PowerPoint (Microsoft, USA). The grid covered the entire visual field from top to bottom (lateral to medial cortex) and was centred over the osteotomy. Grid squares were 160 µm in both directions and intersections, and were then scored as bone, cartilage, fibrous tissue, vascular (red blood cells seen not within tissue matrix), or void based upon haematoxylin and eosin (H&E) uptake and cell morphology for osteoblasts to provide a percentage tissue formation (Figures 3a to 3e). The following parameters were analyzed: 1) total callus area; 2) cartilage volume in callus area; 3) fibrous tissue; 4) mineralized tissue; and 5) osteoblast number.

**Mechanical testing.** Three-point bending tests were performed on excised femora (n = 4 per group). Bone length was measured, and specimens placed horizontally with the anterior surface upwards. A distance of

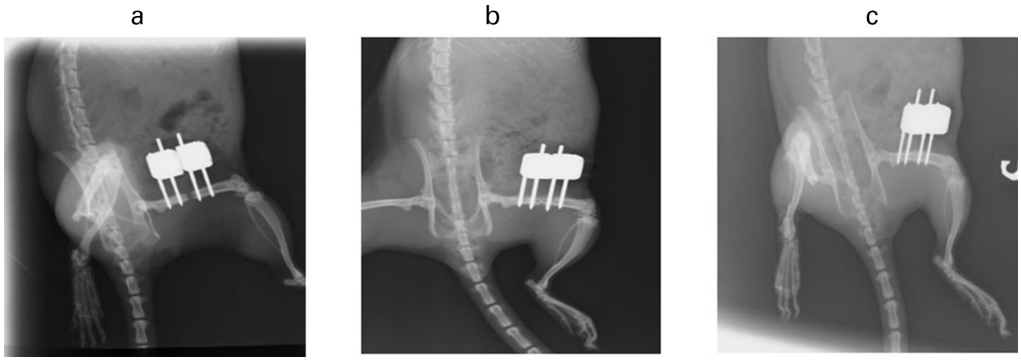


Fig. 4

Radiographs of a fracture site of a rat treated with a high dose combination therapy at: a) day 0; b) three weeks postoperatively; and c) five weeks postoperatively.

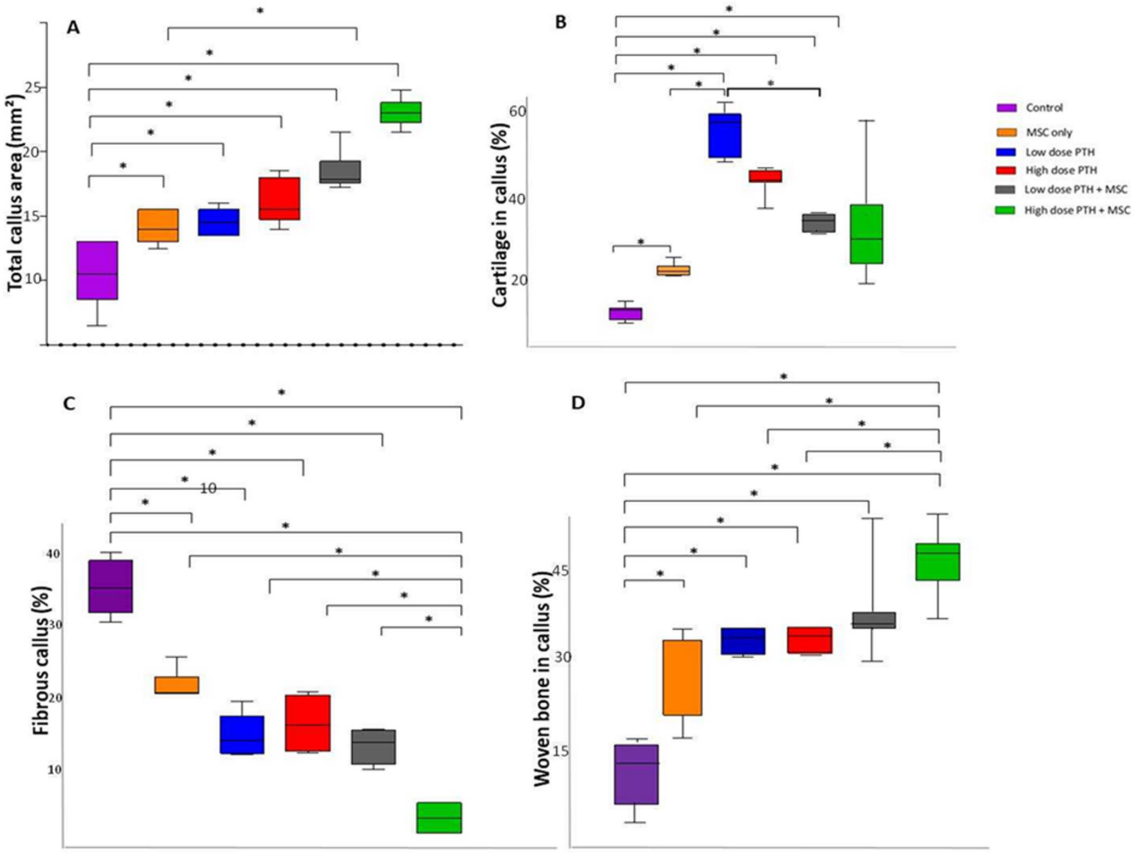


Fig. 5

Histomorphometry of tissues in the fracture gap. a) Total callus area increased in all experimental groups compared to control (*p = 0.039, Mann-Whitney U test). Both low- and high-dose combination therapy showed significantly greater area than mesenchymal stem cells (MSCs) alone and low-dose parathyroid hormone (PTH) alone (*p = 0.051, Mann-Whitney U test). There was no significance between combination therapies and high-dose PTH. b) Percent total callus area that is cartilage. All groups demonstrated a significantly greater percentage than controls *. Low-dose PTH alone demonstrated significantly more cartilage percentage compared to MSCs alone and low-dose combination therapy (*p = 0.041, Mann-Whitney U test). c) Percentage total callus that is fibrous. All groups demonstrated significantly less fibrous tissue than controls (*p = 0.037, Mann-Whitney U test). High-dose combination therapy had a significantly reduced fibrous tissue percentage compared to all other groups (*p = 0.0501, Mann-Whitney U test). d) Percentage total callus that consists of woven bone. All groups had more bone percentage than controls. High-dose combination therapy had significantly more bone than all other groups (*p = 0.041, Mann-Whitney U test) aside from low-dose combination therapy, where there was no statistical difference.

15 mm between the bearing and loading bars for each femur was used as recommended by Turner and Burr.[29] A round-ended indenter with a displacement rate of 5 mm/min was directed vertical to the mid-shaft of the femur to apply a bending load until failure. The failure criterion was defined as a force reduction of 80%. The termination criterion was defined as a force reduction of > 50 N. The test programme was used to determine,

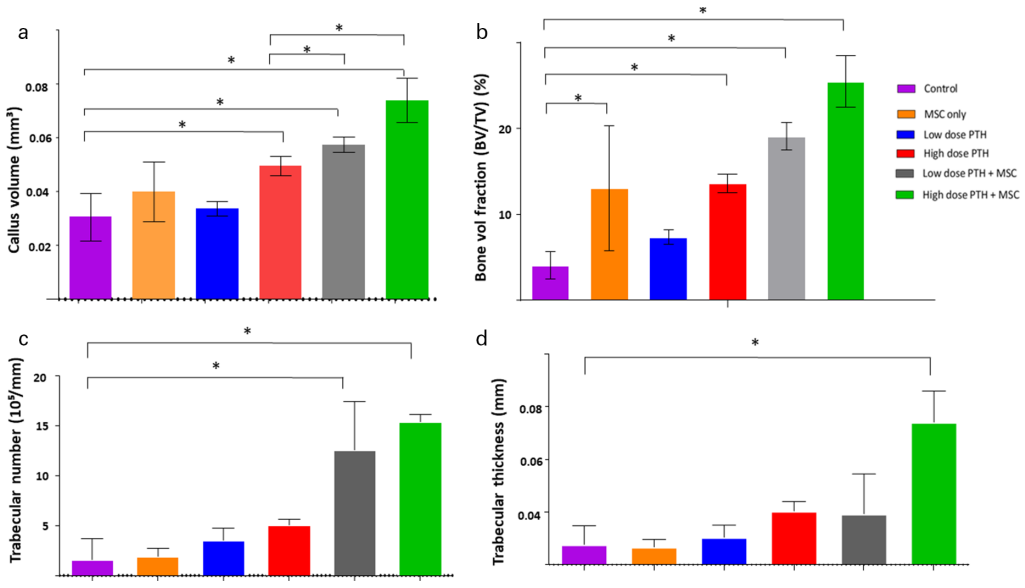


Fig. 6

a) Total callus (bone) volume. Combination therapies and high-dose parathyroid hormone (PTH) demonstrated significant increases in callus volume compared to controls. There was no difference between combination therapies, but they both produced significantly more callus than high-dose PTH (significance represented by *p = 0.050, Mann-Whitney U test). b) The proportion of callus that was bone. This was significantly increased in all groups except for low-dose PTH compared to controls (*p = 0.050, Mann-Whitney U test). High-dose combination produced the greatest bone volume/callus volume (BV/CV) fraction compared to all groups. c) Combination therapies demonstrated significantly increased trabecular number compared to controls (*p = 0.050, Mann-Whitney U test), although no difference was observed between each other. d) High-dose combination therapy only resulted in a significant increase in trabecular thickness compared to control (*p = 0.039, Mann-Whitney U test). MSC, mesenchymal stem cell; TV, trabecular volume.

**Table I.** Ultimate loads and stiffness of treated animals.

| Group | Mean ultimate load, N (SD) | Mean stiffness, N/mm (SD) |
|---|---|---|
| Control fractured | 23 (4.1) | 17 (6) |
| Control unfractured | 64.9 (4.8) | 44.2 (0.8) |
| 25 µg/kg fractured | 34 (3.1) | 28 (6) |
| 25 µg/kg unfractured | 66.1 (5.6) | 41.8 (3.5) |
| 100 µg/kg fractured | 38.6 (4.2) | 26.1 (1.8) |
| 100 µg/kg unfractured | 60.1 (2.1) | 48.7 (5.1) |
| MSCs fractured | 24.5 (11) | 17.6 (9.7) |
| MSCs unfractured | 61.1 (3.9) | 45.9 (1.2) |
| MSC + 25 µg/kg fractured | 44 (1.2) | 31 (2.3) |
| MSC + 25 µg/kg unfractured | 66.4 (8.1) | 48.7 (9.1) |
| MSC + 100 µg/kg fractured | 51 (7.1) | 39.2 (2.8) |
| MSC + 100 µg/kg unfractured | 63.2 (1.2) | 50.7 (5.1) |

MSC, mesenchymal stem cell; SD, standard deviation.

from the load-displacement diagram, the highest point (breaking load (N) and regression (stiffness (N/mm)). The following comparisons in mechanical load were made: 1) differences in contralateral limb across different groups; 2) differences in the fractured limb across different groups; and 3) differences in fractured versus unfractured limb within each group at endpoint.

**Statistical analysis.** Normality was checked using a Shapiro-Wilk test; where the data were non-parametric, comparison were made using Kruskal-Wallis and Mann-Whitney U test with a Bonferroni correction applied (α = 0.05) to compare all the groups. Tests were analyzed with SPSS version 24 (IBM, USA).

## Results

**Radiographs.** The modified RUST score assesses the level of cortical bridging across each cortex on anterior-posterior and lateral radiographs and is scored from 4 to 16. Mean RUST score was significantly greater for all treatment groups compared to controls at five weeks (p = 0.049, Mann-Whitney U test). High-dose combination therapy demonstrated the greatest mean score (13.8 (standard deviation (SD) 1.3)) (p = 0.048, Mann-Whitney U test), followed by low-dose combination therapy (10.1 (SD 0.8)) (p = 0.041, Mann-Whitney U test). There was no significant difference between mean high-dose PTH (7.8 (SD 1.1)) and MSCs alone (7.1 (SD 0.9)) (p = 0.817, Mann-Whitney U test) (control 5.8 (SD 0.5)) (Figure 4).

**Histology and histomorphometry: total callus area.** The combination therapy groups demonstrated the greatest total callus area compared to all other groups (p = 0.039, Mann-Whitney U test). Similarly, high-dose PTH, low-dose PTH, and MSCs alone also demonstrated significantly greater callus area compared to controls (p = 0.051, Mann-Whitney U test). Low-dose PTH+ MSC showed significantly greater callus than MSCs alone, and low PTH alone (p = 0.049, Mann-Whitney U test). Although the medial values for the total callus area was highest with the high-dose MSC combination, there was

no significant difference between low-dose PTH+ MSC and high-dose PTH alone (p = 0.079, Mann-Whitney U test) (Figure 5a).

**Cartilage volume in callus area.** The low-dose PTH group had the greatest mean cartilage volume (54.1% (SD 1.2)) compared to controls (19.2% (SD 0.7)) (p = 0.041, Mann-Whitney U test). All groups produced more cartilage than controls. There was marked variability in the mean amount of cartilage produced by the high-dose combination group (32% (SD 29.1)), more so than any other group. Because of this, there was no significant difference between this group and low-dose combination (mean 38.9% (SD 0.9)). MSCs alone produced the least cartilage of any treatment group compared to controls (mean 29% (SD 7.1)) (Figure 5b).

**Fibrous tissue.** Controls demonstrated the greatest mean percentage of fibrous tissue within the fracture gap (46.1% (SD 11.8%)) (p = 0.037, Mann-Whitney U test), equating to a fibrous nonunion as correlated with the low RUST scores. There was no significant difference in the mean percentage of fibrous tissue in the callus between MSCs alone (21.4% (SD 18.1%)), high-dose PTH (19.8% (SD 4.4%)), low-dose PTH (18.1% (SD 9.1%)), or low-dose combination (17.6% (SD 11.1%)), but high-dose combination produced significantly less mean fibrous tissue within the fracture gap than any other group (11.9% (SD 2.3%)) (p = 0.0501, Mann-Whitney U test) (Figure 5c).

**Mineralized tissue.** All groups demonstrated significantly more mineralized tissue than controls (mean 19.1% (SD 11.8)). The high-dose combination (mean 49.1 (SD 7.2)) had significantly more woven bone than high-dose PTH alone (mean 34.8 (SD 1.4)), low-dose PTH alone (mean 35.6 (SD 6.2)), and MSCs alone (mean 32.1 (SD 8.1)) (p = 0.049, Mann-Whitney U test) (Figure 5d).

**Osteoblast number.** The high-dose combination group had the greatest mean increase in osteoblast number within the callus compared to controls (p = 0.031, Mann-Whitney U test), followed by low-dose combination, high-dose PTH, MSCs alone, and then low-dose PTH (p = 0.046, Mann-Whitney U test).

**Allen score.** The Allen score of the high-dose combination PTH group was the most significantly increased compared to the control (p = 0.037, Mann-Whitney U test) (mean 4.75 (SD 0.8) vs 2.65 (SD 1.2)). However, again there was no difference between high- and low-dose combination therapies (p = 0.074, Mann-Whitney U test).

**Micro-CT: total bone volume.** Mean total bone volume was significantly increased in both combination therapy groups (high combination 0.09 $mm^3$ (SD 0.01) and low combination 0.07 $mm^3$ (SD 0.02)) and high-dose PTH alone (0.05 $mm^3$ (SD 0.02)) compared to controls (0.03 $mm^3$ (SD 0.02)) (p = 0.050, Mann-Whitney U test). There was no significant difference in the MSCs alone group (0.03 $mm^3$ (SD 0.03)) (p = 0.069, Mann-Whitney U test). The combination therapy groups produced significantly more bone volume than the high-dose PTH alone group (p = 0.037, Mann-Whitney U test) (Figure 6a).

**Bone volume fraction.** All groups demonstrated increased bone volume fraction compared to controls (p = 0.050, Mann-Whitney U test), except low dose PTH alone (p = 0.059, Mann-Whitney U test). High-dose combination therapy produced the greatest mean bone volume fraction (28.1% (SD 3.6%)), followed by low-dose combination therapy (18% (SD 0.9%)) (Figure 6b).

**Trabecular number and thickness.** Both high- and low-dose combination therapy led to an increase in mean TbN (13.8/mm (SD 1.8) and 12.6/mm (SD 0.7), respectively) (p = 0.050, Mann-Whitney U test), although only high-dose combination therapy significantly increased mean TbTh (0.07 mm (SD 3.45)) (p = 0.039, Mann-Whitney U test) compared to controls (TbN 3.6/mm (SD 0.79) and TbTh 0.03 mm (SD 1.66)). There was no significant difference between the combination therapies with regards to trabecular parameters (p = 0.97) (Figures 6c and 6d).

**Mechanical testing.** On review of the contralateral unfractured limb, high-dose PTH alone and high-dose combination therapy groups demonstrated significantly increased stiffness and ultimate load to failure compared to controls (p = 0.049, Mann-Whitney U test). There was no difference in ultimate load or stiffness of the unfractured limbs of samples taken from low-dose PTH, MSCs alone, or low-dose combination therapy groups compared to controls (Table I).

For the fractured limbs, no significant difference was found between the mechanical characteristics of MSCs alone and controls. Interestingly, low-dose PTH alone had no effect on stiffness compared to controls, but did show a greater ultimate load to failure (p = 0.049, Mann-Whitney U test) (Table I). Within each group, the unfractured limbs had significantly greater ultimate load to failure and stiffness compared to their respective fractured limbs (p = 0.050, Mann-Whitney U test).

## Discussion

Our study has demonstrated enhancement of fracture healing with combination therapy of MSCs and PTH administered concurrently, compared to control animals, although there was not always a significant difference in the various parameters that were measured between high- and low-dose combination groups. Both combination therapies led to an increase in TbN, although only high-dose combination therapy increased TbTh. This translated to significant improvements in mechanical stiffness and ultimate load to failure point in both combination therapy groups. We observed more mineralized tissue and greater mechanical integrity at the fracture site with combination therapies compared to PTH or MSCs alone.

The increase in bone volume in animals treated with PTH alone was not a result of improvements in bone microarchitecture, with no significant changes in trabecular parameters; this is also true of MSC-alone groups.

Conversely, combination therapy groups both lead to an increase in TbN, while high-dose combination therapy also caused increased TbTh. This disparity between TbTh and TbN is due to greater callus integrity/maturity in the high-dose combination group. On the contrary, the increase in callus area, compared to controls in the MSC-alone groups, was due to an equal increase in woven bone and cartilage percentage and did not translate to significant improvements in mechanical integrity.

Our study demonstrated a dose dependency of PTH use on its own in relation to callus maturity and mechanical characteristics. This is similar to other studies investigating fracture healing in rodent models. The literature still remains inconsistent regarding the best dosing concentration for bone formation in the fracture context. Rodent study dosing is typically 4 to 40 µg/kg per day,[30] while approved human dosing is 20 mg/day, which in rats is approximately equivalent to 0.3 to 0.5 µg/kg/day.[31] Nonetheless, the unclear receptor binding profile in rodents means the administered high dose may not be wholly absorbed or active, and therefore the acting dose may be much lower than the concentration administered.[32] Alkhiary et al[4] investigated healing in rats with 5 and 30 µg/kg of PTH, finding greater bone formation at the higher concentration. Similarly, Milstrey et al[33] compared fracture healing at 10, 40, and 200 µg/kg, finding improved bone formation at higher concentrations, but no changes to mechanical stiffness. Conversely, Andreassen et al[2] found no difference in fracture healing between 60 and 20 µg/kg after 40 days. Yet, the doses in these studies were much higher than the clinical dose used in osteoporosis treatment. At lower doses, Nakajima et al[3] and Chen et al[34] reported that daily treatment led to an increase of osteoclasts, ALP, and osteocalcin within three weeks after femoral fracture, and also increased the mechanical strength and bone mineral density (BMD) of the callus at six weeks. We also confirmed a positive effect of the low-dose PTH alone, as well as in combination with MSCs, but in nearly all parameters this was not as significant as high-dose PTH alone or in combination.

Importantly, the consistency of our PTH findings, and the magnitude of the improvements seen with combination groups, validate the decision to use a five-day Monday to Friday dosing. Our study had one end point at 35 days, and increases specific to endochondral ossification may have been missed by not having a 14-day marker. Therefore, an earlier timepoint would have answered the question of enhancement versus acceleration.

The use of MSCs in preclinical trials has been well documented.[35,36] Although clinically MSCs have been used locally in the healing of nonunions, particularly tibial and calcaneal, and pre-clinical work has investigated their administration systemically, to migrate to sites of bone injury, very few studies have used cells in combination with PTH to enhance fracture healing. Sheyn et al[19] used intravenous MSCs and teripratide to improve vertebral fracture healing, noting that the additive method enhanced bone formation, and promoted the terminal differentiation of cells down the osteoplastic lineage. The same group reported similar findings in the setting of multiple anterior rib fractures.[18] Our findings support the utility of combining these methods, but we are the first to do so in a weightbearing limb and using locally injected MSCs. Local administration overcomes issues that may arise from microvascular retention within the respiratory or hepatic systems or aberrant migration of cells to other locations instead of the site of injury.

Although the majority of fractures heal without biological interventions, a growing proportion in geriatric populations and those sustained at high energy would benefit from enhanced or accelerated union; as such we highlight local administration of MSCs in combination with systemic PTH as a therapy worthy of greater exploration.

## Supplementary material

An ARRIVE checklist is included to show that the ARRIVE guidelines were adhered to in this study.

## References


1. **Neer RM**, **Arnaud D**, **Zanchetta JR**, **et al**. Effect of parathyroid hormone(1-34)on fractures and bone mineral density in postmenopausal women with osteoporosis. *N Engl J Med*. 2001;344(19):1434–1441.
2. **Andreassen TT**, **Ejersted C**, **Oxlund H**. Intermittent parathyroid hormone(1-34) treatment increases callus formation and mechanical strength of healing rat fractures. *J Bone Miner Res*. 1999;14(6):960–968.
3. **Nakajima A**, **Shimoji N**, **Shiomi K**, **et al**. Mechanisms for the enhancement of fracture healing in rats treated with intermittent low-dose human parathyroid hormone (1-34). *J Bone Miner Res*. 2002;17(11):2038–2047.
4. **Alkhiary YM**, **Gerstenfeld LC**, **Krall E**, **et al**. Enhancement of experimental fracture-healing by systemic administration of recombinant human parathyroid hormone (PTH 1-34). *J Bone Joint Surg Am*. 2005;87-A(4):731–741.
5. **Barnes GL**, **Kakar S**, **Vora S**, **Morgan EF**, **Gerstenfeld LC**, **Einhorn TA**. Stimulation of fracture-healing with systemic intermittent parathyroid hormone treatment. *J Bone Joint Surg Am*. 2008;90 Suppl 1:120–127.
6. **Campbell EJ**, **Campbell GM**, **Hanley DA**. The effect of parathyroid hormone and teriparatide on fracture healing. *Expert Opin Biol Ther*. 2015;15(1):119–129.
7. **Aspenberg P**, **Genant HK**, **Johansson T**, **et al**. Teriparatide for acceleration of fracture repair in humans: a prospective, randomized, double-blind study of 102 postmenopausal women with distal radial fractures. *J Bone Miner Res*. 2010;25(2):404–414.
8. **Iwata A**, **Kanayama M**, **Oha F**, **Hashimoto T**, **Iwasaki N**. Effect of teriparatide(rh-PTH 1-34) versus bisphosphonate on the healing of osteoporotic vertebral compression fracture:a retrospective comparative study. *BMC Musculoskelet Disord*. 2017;18(1):148.
9. **Nauth A**, **Giannoudis PV**, **Einhorn TA**, **et al**. Growth factors: beyond bone morphogenetic proteins. *J Orthop Trauma*. 2010;24(9):543–546.
10. **Peichl P**, **Holzer LA**, **Maier R**, **Holzer G**. Parathyroid hormone 1-84 accelerates fracture-healing in pubic bones of elderly osteoporotic women. *J Bone Joint Surg Am*. 2011;93-A(17):1583–1587.
11. **Zhang D**, **Potty A**, **Vyas P**, **Lane J**. The role of recombinant PTH in human fracture healing: a systematic review. *J Orthop Trauma*. 2014;28(1):57–62.
12. **Bhandari M**, **Jin L**, **See K**, **et al**. Does teriparatide improve femoral neck fracture healing: Results from a randomized placebo-controlled trial. *Clin Orthop Relat Res*. 2016;474(5):1234–1244.
13. **Johansson T**. PTH 1-34 (teriparatide) may not improve healing in proximal humerus fractures. A randomized, controlled study of 40 patients. *Acta Orthop*. 2016;87(1):79–82.
14. **Kim SM**, **Kang KC**, **Kim JW**, **Lim SJ**, **Hahn MH**. Current role and application of teriparatide in fracture heant Role and Application of Teriparatide in Fracture Healing of Osteoporotic Patients: A Systematic Review. *J Bone Metab*. 2017;24(1):65–73.
15. **Homma Y**, **Zimmermann G**, **Hernigou P**. Cellular therapies for the treatment of non-union: the past, present and future. *Injury*. 2013;44(Suppl 1):S46-9.
16. **Jäger M**, **Herten M**, **Fochtmann U**, **et al**. Bridging the gap: bone marrow aspiration concentrate reduces autologous bone grafting in osseous defects. *J Orthop Res*. 2011;29(2):173–180.

17. **Hernigou P**, **Dubory A**, **Flouzat Lachaniette CH**, **Khaled I**, **Chevallier N**, **Rouard H**. Stem cell therapy in early post-traumatic talus osteonecrosis. *Int Orthop*. 2018;42(12):2949–2956.
18. **Cohn Yakubovich D**, **Sheyn D**, **Bez M**, **et al**. Systemic administration of mesenchymal stem cells combined with parathyroid hormone therapy synergistically regenerates multiple rib fractures. *Stem Cell Res Ther*. 2017;8(1):51.
19. **Sheyn D**, **Shapiro G**, **Tawackoli W**, **et al**. PTH induces systemically administered mesenchymal stem cells to migrate to and regenerate spine injuries. *Mol Ther*. 2016;24(2):318–330.
20. **Lee OK**, **Coathup MJ**, **Goodship AE**, **Blunn GW**. Use of mesenchymal stem cells to facilitate bone regeneration in normal and chemotherapy-treated rats. *Tissue Eng*. 2005;11(11–12):1727–1735.
21. **Osagie-Clouard L**, **Sanghani-Kerai A**, **Coathup M**, **Meeson R**, **Briggs T**, **Blunn G**. The influence of parathyroid hormone 1-34 on the osteogenic characteristics of adipose- and bone-marrow-derived mesenchymal stem cells from juvenile and ovarectomized rats. *Bone Joint Res*. 2019;8(8):397–404.
22. **Meeson R**, **Moazen M**, **Sanghani-Kerai A**, **Osagie-Clouard L**, **Coathup M**, **Blunn G**. The influence of gap size on the development of fracture union with a micro external fixator. *J Mech Behav Biomed Mater*. 2019;99:161–168.
23. **Meeson R**, **Sanghani-Keri A**, **Coathup M**, **Blunn G**. CXCR4 Antagonism to Treat Delayed Fracture Healing. *Tissue Eng Part A*. 2019;25(17–18):1242–1250.
24. **Chamieh F**, **Collignon A-M**, **Coyac BR**, **et al**. Accelerated craniofacial bone regeneration through dense collagen gel scaffolds seeded with dental pulp stem cells. *Sci Rep*. 2016;6:38814.
25. **Litrenta J**, **Tornetta P**, **Mehta S**, **et al**. Determination of radiographic healing: An assessment of consistency using rust and modified rust in metadiaphyseal fractures. *J Orthop Trauma*. 2015;29(11):516–520.
26. **Whelan DB**, **Bhandari M**, **Stephen D**, **et al**. Development of the radiographic union score for tibial fractures for the assessment of tibial fracture healing after intramedullary fixation. *J Trauma*. 2010;68(3):629–632.
27. **Lane JM**, **Sandhu HS**. Current approaches to experimental bone grafting. *Orthop Clin North Am*. 1987;18(2):213–225.
28. **Allen HL**, **Wase A**, **Bear WT**. Indomethacin and aspirin:effect of nonsteroidal anti-inflammatory agents on the rate of fracture repair in the rat. *Acta Orthop Scand*. 1980;51(4):595–600.
29. **Turner CH**, **Burr DB**. Basic biomechanical measurements of bone: a tutorial. *Bone*. 1993;14(4):595–608.
30. **Kim KM**, **Lee SY**, **Rhee Y**. Influence of dosing interval and administration on the bone metabolism, skeletal effects, and clinical efficacy of parathyroid hormone in treating osteoporosis: a narrative review. *JBMR Plus*. 2017;1(1):36–45.
31. **Tashjian AH**, **Chabner BA**. Commentary on clinical safety of recombinant human parathyroid hormone 1-34 in the treatment of osteoporosis in men and postmenopausal women. *J Bone Miner Res*. 2002;17(7):1151–1161.
32. **Mannstadt M**, **Jüppner H**, **Gardella TJ**. Receptors for PTH and PTHrP: their biological importance and functional properties. *Am J Physiol*. 1999;277(5):F665-75.
33. **Milstrey A**, **Wieskoetter B**, **Hinze D**, **et al**. Dose-dependent effect of parathyroid hormone on fracture healing and bone formation in mice. *J Surg Res*. 2017;220:327–335.
34. **Chen Y**, **Liu R**, **Hettinghouse A**, **Wang S**, **Liu G**, **Liu CJ**. Clinical Application of Teriparatide in Fracture Prevention: A Systematic Review. *JBJS Rev*. 2019;7(1):e10.
35. **Altman AR**, **Tseng WJ**, **de Bakker CMJ**, **et al**. Quantification of skeletal growth, modeling, and remodeling by in vivo micro computed tomography. *Bone*. 2015;81:370–379.
36. **Sanghani A**, **Osagie-Clouard L**, **Samizadeh S**, **et al**. CXCR4 Has the Potential to Enhance Bone Formation in Osteopenic Rats. *Tissue Eng Part A*. 2018;24(23–24):1775–1783.



**Author information:**
- L. Osagie-Clouard, MBBS, PhD, Trauma and Orthopedic Registrar
- R. Meeson, MA VetMB, PhD, MVetMed DipECVS, PGCE(VetEd) FHEA FRCVS, Head of Orthopaedic Surgery & Senior Lecturer
- A. Sanghani-Kerai, MEng, PhD, Biomedical Engineer
- T. Briggs, MBBS, Consultant Orthopaedic Surgeon
  Royal National Orthopaedic Hospital, London, UK.
- M. Bostrom, MD, Specialist in knee and hip surgery, Hospital for Special Surgery, New York, New York, USA.
- G. Blunn, PhD, Professor of Bioengineering, School of Pharmacy and Biomedical Sciences, University of Portsmouth, Portsmouth, UK.



**Author contributions:**
- L. Osagie-Clouard: Data curation, Formal analysis, Investigation, Writing – original draft, Writing – review & editing, Funding acquisition.
- R. Meeson: Methodology, Validation, Visualization, Writing – review & editing.
- A. Sanghani-Kerai: Investigation, Methodology, Writing – review & editing.
- M. Bostrom: Funding acquisition, Supervision, Writing – review & editing.
- T Briggs:Supervision, Writing – review & editing, Conceptualization
- G. Blunn: Conceptualization, Funding acquisition, Supervision, Writing – review & editing, Methodology, Project administration.

**Funding statement:**
- No benefits in any form have been received or will be received from a commercial party related directly or indirectly to the subject of this article.

**ICMJE COI statement:**
- M. Bostrom reports unpaid board membership on the Hip Society and the American Austrian Foundation, consultancy payments and royalties from Smith and Nephew, and grants from Smith and Nephew and Ines Mandl Research Foundation. G. Blunn reports an institutional grant from Dunhill Medical Trust for this study. T. Briggs reports board membership on Native Technology Ltd, payment for medicolegal expert testimony, and royalties from medical textbooks, all unrelated to the study.

**Open access funding:**
- The authors confirm that the open access fees for this study was funded by Rosetree's trust.